Author(s):	Ilmarinen, Tanja; Hiidenmaa, Hanna; Kööbi, Peeter; Nymark, Soile; Sorkio, Anni; Wang, Jing-Huan; Stanzel, Boris V; Thieltges, Fabian; Alajuuma, Päivi; Oksala, Olli; Kataja, Marko; Uusitalo, Hannu; Skottman, Heli
Title:	Ultrathin Polyimide Membrane as Cell Carrier for Subretinal Transplantation of Human Embryonic Stem Cell Derived Retinal Pigment Epithelium
Year:	2015
Journal Title:	Plos ONE
Vol and number:	10 : 11
Pages:	1-18
ISSN:	1932-6203
Discipline:	Biomedicine; Otorhinolaryngology, ophthalmology
School /Other Unit:	BioMediTech; School of Medicine
Item Type:	Journal Article
Language:	en
DOI:	http://dx.doi.org/10.1371/journal.pone.0143669
URN:	URN:NBN:fi:uta-201512152550
URL:	http://dx.doi.org/10.1371/journal.pone.0143669

PLOS | ONE

RESEARCH ARTICLE

Ultrathin Polyimide Membrane as Cell Carrier for Subretinal Transplantation of Human Embryonic Stem Cell Derived Retinal Pigment Epithelium

Tanja Ilmarinen[1]*, Hanna Hiidenmaa[1], Peeter Kööbi[2], Soile Nymark[3], Anni Sorkio[1], Jing-Huan Wang[2], Boris V. Stanzel[4], Fabian Thieltges[4], Päivi Alajuuma[5], Olli Oksala[5], Marko Kataja[6], Hannu Uusitalo[2], Heli Skottman[1]

1 BioMediTech, University of Tampere, Tampere, Finland, **2** Department of Ophthalmology, SILK, University of Tampere and Tays Eye Center, Tampere, Finland, **3** Department of Electronics and Communications Engineering and BioMediTech, Tampere University of Technology, Tampere, Finland, **4** Department of Ophthalmology, University of Bonn, Bonn, Germany, **5** Santen Oy, Tampere, Finland, **6** Tays Eye Center, Tampere, Finland

* tanja.ilmarinen@uta.fi

OPEN ACCESS

Citation: Ilmarinen T, Hiidenmaa H, Kööbi P, Nymark S, Sorkio A, Wang J-H, et al. (2015) Ultrathin Polyimide Membrane as Cell Carrier for Subretinal Transplantation of Human Embryonic Stem Cell Derived Retinal Pigment Epithelium. PLoS ONE 10 (11): e0143669. doi:10.1371/journal.pone.0143669

Editor: Majlinda Lako, University of Newcastle upon Tyne, UNITED KINGDOM

Received: September 2, 2015

Accepted: November 6, 2015

Published: November 25, 2015

Data Availability Statement: All relevant data are within the paper and its Supporting Information files.

Funding: Santen Oy provided support in the form of salaries for authors [PA OO]. The specific roles of these authors are articulated in the 'author contributions' section. In addition, Santen Oy paid the animal costs and part of reagent costs. Santen Oy did not have any additional role in the study design, data collection and analysis, decision to publish, or preparation of the manuscript. Päivikki and Sakari Sohlberg Foundation, (www.pss-saatio.fi) (HS); The Finnish funding agency of innovation, (www.tekes.fi),

Abstract

In this study, we investigated the suitability of ultrathin and porous polyimide (PI) membrane as a carrier for subretinal transplantation of human embryonic stem cell (hESC) -derived retinal pigment epithelial (RPE) cells in rabbits. The *in vivo* effects of hESC-RPE cells were analyzed by subretinal suspension injection into Royal College of Surgeons (RCS) rats. Rat eyes were analyzed with electroretinography (ERG) and histology. After analyzing the surface and permeability properties of PI, subretinal PI membrane transplantations with and without hESC-RPE were performed in rabbits. The rabbits were followed for three months and eyes analyzed with fundus photography, ERG, optical coherence tomography (OCT), and histology. Animals were immunosuppressed with cyclosporine the entire follow-up time. In dystrophic RCS rats, ERG and outer nuclear layer (ONL) thickness showed some rescue after hESC-RPE injection. Cells positive for human antigen were found in clusters under the retina 41 days post-injection but not anymore after 105 days. In rabbits, OCT showed good placement of the PI. However, there was loss of pigmentation on the hESC-RPE-PI over time. In the eyes with PI alone, no obvious signs of inflammation or retinal atrophy were observed. In the presence of hESC-RPE, mononuclear cell infiltration and retinal atrophy were observed around the membranes. The porous ultrathin PI membrane was well-tolerated in the subretinal space and is a promising scaffold for RPE transplantation. However, the rejection of the transplanted cells seems to be a major problem and the given immunosuppression was insufficient for reduction of xenograft induced inflammation.

grant numbers 866/31/2009 and 549/31/2011 (HS); the Academy of Finland, (www.aka.fi), grant numbers 218050 (HS), 133879 (TI), and 260375 (SN); the Finnish Cultural Foundation, (www.skr.fi), grant number 130858 (AS); Tampere Graduate Program in Biomedicine and Biotechnology, (www.uta.fi/bmt/doctoral_programme.html) (HH); BONFOR/Gerok Scholarship, (www.ukb.uni-bonn.de/quick2web/internet/internet.nsf/vwUNIDLookup/B72A5EAAF5CFF627C1257658002584DA), grant number O-137.0019 (BS and FT); the Emil Aaltonen Foundation, (www.emilaaltonen.fi), (SN). None of the funders had any role in study design, data collection and analysis, decision to publish, or preparation of the manuscript.

Competing Interests: PA and OO are employed by Santen Oy. This project was partly funded by TEKES, which requires shared funding with industrial partners. In this study the commercial partner was Santen Oy. This commercial affiliation has not influenced the performance or presentation of the work described in this manuscript.

Introduction

Retinal pigment epithelium (RPE) is a monolayer of cells between the neural retina and the choriocapillaris. It is vital as part of the blood-retina-barrier. It also supports photoreceptor function and survival by providing nutrients, absorbing stray light, phagocytosing photoreceptor outer segments, and controlling regeneration of visual pigments, ion flow, and oxidative stress [1].

RPE degeneration has a major role in pathogenesis of retinal diseases including age-related macular degeneration (AMD), a leading cause of blindness in developed societies [2]. In AMD, local degeneration of RPE eventually leads to death of photoreceptors [3]. A promising future treatment for AMD is cell therapy and submacular transplantation of RPE, which has been studied extensively [4]. Human pluripotent stem cells (hPSCs) are potential and readily available source for RPE replacement [5, 6]. Recent stem cell -based clinical trials for RPE-related diseases aim to establish safety and dosing with RPE cell suspensions derived from human embryonic stem cells (hESCs) [7, 8]. However, concerns remain that suspended RPE may fail to survive or function in the long-term on the diseased Bruch's membrane [9, 10]. Another approach under clinical trial in Japan is transplantation of autologous human induced pluripotent stem cell (hiPSC) -derived RPE sheets without a supporting artificial scaffold [11, 12].

Biomaterial based carriers could facilitate surgical handling of intact RPE and ensure better long-term function of the transplanted cells [11–13]. Several materials have been proposed for RPE transplantation [14–17]. However, to date, transplantations of human RPE-scaffolds have been reported only with adult and fetal RPE cells on polyester in rabbits [18, 19] and with hPSC-RPE cells on parylene-C in rats [13, 20]. Despite encouraging results, further studies are needed to improve the biocompatibility of the scaffolds. One potential material is synthetic polymer polyimide (PI). Depending on its structure, PI has been clinically approved and its ocular biocompatibility has been demonstrated [21, 22]. Previously, PI membranes have been tested for subretinal transplantation in rats and pigs [23, 24]. We have also demonstrated that PI supports culture of hESC-RPE [25].

In this study, we aimed to further characterize the suitability of ultrathin and porous PI for subretinal transplantation of hESC-RPE. First, we assessed the *in vivo* effects of the hESC-RPE cells by injecting them subretinally in Royal College of Surgeons (RCS) rats, an FDA approved animal model for retinal degeneration [26]. For PI membrane transplantations, a larger eyed animal model rabbit was chosen for evaluation of surgical feasibility of the membrane. To our knowledge, this is the first report of *in vivo* studies with hPSC-RPE-biomaterial sheet transplantation in larger animals.

Materials and Methods

Surface and permeability characterization of ultrathin PI membrane

The properties of ultrathin (7.6 μm) PI membranes (pore diameter 1 μm, pore density 2.2 x 10^7 pores/cm^2; it4ip, Seneffe, Belgium) were examined with scanning electron microscopy (SEM), atomic force microscopy (AFM), contact angle analysis, and Ussing chamber system. A commonly used RPE culture substrate, polyethylene terephthalate (PET) membrane, was analyzed for comparison.

The pore distributions were determined by SEM (Quanta 3D, FEI, UK) operating at 5 kV. Samples were sputter coated with a thin layer of gold, using an Emitech K500X (Quorum Technologies, UK) to reduce charging and image distortion.

AFM (Nanoscope Dimension 3100, Vecco, USA) was equipped with a TESPA silicon tip (Vecco) mounted on a cantilever of stiffness of 20–80 N/m^{-1}, operating at a resonance of 300

Hz and a scan rate of 0.996 Hz. Images were acquired in tapping mode. Root mean square average (Rq) values were calculated from 12 scan areas of 2 μm x 2 μm. Images were analyzed with the Nanoscope 6.11r1 Software (Vecco).

Static contact angle (CAM2000, KSV Instrument Ltd., Finland) measurements were taken using a 5 μl drop of Milli-Q water. Ten to 13 readings were performed per membrane type.

Flux of a small molecular weight (700 Da) Alexa Fluor® 568 Hydrazide sodium salt (Life Technologies, Paisley, UK) at a concentration of 0.0065 mM was measured in Ussing chamber system (Physiologic Instruments, San Diego, CA) as described previously [16]. Samples were collected from the receptor chamber at 60, 120, 180 and 240 min. The diffusion of Alexa Fluor® 568 Hydrazide sodium salt across the membranes was characterized by calculating the apparent permeability coefficient (Papp, cm^2s^{-1}) as Papp = dC/dt/(60C0A), where dC/dt is the slope of the linear portion of the permeability curve, C0 is the initial concentration in the donor chamber, and A is the exposed surface area of the hESC-RPE monolayer (0.031 cm^2). The cumulative permeability demonstrates the percentage of diffused fluorescent marker in the receptor chamber compared to initial concentration in the donor chamber over time.

Culture of hESC lines and RPE differentiation

The National Authority for Medicolegal Affairs Finland has approved our research with human embryos (Dnro 1426/32/300/05). We also have a supportive statement from the local ethics committee of the Pirkanmaa hospital district Finland to derive and expand hESC lines for research purposes (R05116).

Human ESC lines Regea08/023 and Regea08/017, which were previously derived in our laboratory [27], were cultured as previously described [28]. The hESC-RPE differentiation was performed spontaneously in floating cell clusters using RPEbasic method as described previously [28]. For enrichment, the pigmented areas were isolated manually using a scalpel. Subsequently, cells were dissociated with 1x Trypsin-EDTA (Lonza, Basel, Switzerland) or Tryple Select (Life Technologies), filtered through 40 μm cell strainer (BD Biosciences, NJ, USA), and seeded 160 000–200 000 cells/cm^2 on collagen IV -coated (human placenta, 5 μg/cm^2; Sigma-Aldrich, MO, USA) 24-well plates (NUNC, Thermo Fisher Scientific, Tokyo, Japan). After enrichment, the pigmented cells were replated on collagen IV -coated (5 μg/cm^2) 24-well plates from which the cells were dissociated for injections. For PI membrane transplantation, the cells were replated on laminin-coated (human placenta, 10 μg/cm^2; Sigma-Aldrich) PI.

Transplantation studies

All animal experiments were approved by the Finnish National Animal Experiment Board (STH832A and PH398A) and the state regulatory authorities of North Rhine-Westphalia (LANUV 84–02.04.2014.A082), and were performed in accordance with the ARVO Statement for the Use of Animals in Ophthalmic and Vision research. All efforts were made to minimize suffering. The animals were maintained in temperature controlled environment in a 12 h light-dark cycle with free access to water.

Cell suspension injection

These protocols have been described in detail in S1 Materials and Methods.

Prior injection, the expression of RPE/eye-related genes and proteins were analyzed from the hESC-RPE cells with reverse transcription polymerase chain reaction (RT-PCR) and immunocytochemistry. Passage three hESC-RPE cells (100 000 cells per injection) were used for subretinal injections into dystrophic and non-dystrophic RCS rats. The study groups were 1) no injection (n = 1 eye/rat strain), 2) injection of RPEbasic medium without cells (n = 1 eye/

rat strain), 3) injection of hESC-RPE in RPEbasic medium (n = 4 eyes/dystrophic and n = 3 eyes/non-dystrophic). The viability of cells left over from injections and kept in suspension for 6 h at +4°C was analyzed with LIVE/DEAD® Cell Viability Assay kit (Life Technologies).

PI membrane transplantation

For PI membrane transplantation, 1 × 4 mm bullet shaped implants were manually cut with a scalpel from laminin-coated PI membranes without and with hESC-RPE. The membranes were kept at +37°C until transplanted.

Nine albino New Zealand White rabbits weighing 3.1–3.9 kg were used. Due to the long follow-up time, systemic administration of immunosuppressant was chosen instead of repeated intraocular injections. The rabbits received 25 mg/kg cyclosporin A (Novartis, Basel, Switzerland) in drinking water starting two days before the transplantation until the end of follow-up (three months). The volume of water consumed by the animals was recorded daily. The rabbits were anesthetized with an intramuscular injection of 5 mg/kg xylazine (Bayer AG, Leverkusen, Germany) and 25 mg/kg ketamine (Parke-Davis Scandinavia AB, Solna, Sweden). Anesthesia was maintained with intravenously administered xylazine/ketamine. Topical anesthesia was performed with oxybuprocaine hydrochloride (Santen, Osaka, Japan) and the pupils were dilated with tropicamid (Santen) and 2.5% phenylephrine hydrochloride (Bausch & Lomb, NJ, USA).

Limbal conjunctival openings and 20 gauge sclerotomies were made into inferotemporal, inferonasal and superior segments of the right eye for infusion cannula, endoillumination, and other surgical instrumentation, respectively. Partial vitrectomy was performed using Accurus vitrectomy system (Alcon Laboratories, TX, USA). A small posterior retinotomy was made using 27 gauge injection needle tip and a small retinal bleb was gently raised by injecting balanced salt solution (BSS) into subretinal space. PI membrane alone (n = 3) or with hESC-RPE cells (hESC-RPE-PI, n = 5) was placed into subretinal space via superior sclerotomy and retinotomy using 23 gauge Grieshaber forceps (Alcon Labs, TX, USA). Retinal bleb was then reattached by passive aspiration of subretinal fluid via silicone tip 20 gauge cannula and vitreous cavity filled with 5000-centistoke silicone oil. Sclerotomies and conjunctival openings were closed using 7–0 Vicryl sutures. One animals underwent surgery without delivery of PI membrane (surgical control).

In order to better protect the hESC-RPE on PI and aid surgical manageability of the membrane, we evaluated the suitability of a custom-made shooter instrument [19] for delivery of ultrathin PI into the subretinal space of rabbits (n = 6, pigmented chinchilla bastard, >1.5kg), according to previously published surgical techniques [18]. In brief, following a 2 port 23G vitrectomy with the Mach 2 cutter attached to a Megatron S4 MPS device and 25G chandelier illumination connected to a Xenotron 3 light machine (all Geuder SG, Heidelberg, Germany), which included manual induction of posterior vitreous detachment, the surgeon (BVS) attempted to pass implants without cells through an enlarged retinotomy in a bleb retinal detachment into the subretinal space.

Post-transplantation analyses

Electroretinography (ERG) measurements and optical coherence tomography (OCT) imaging. Dark-adapted Ganzfeld ERGs were recorded under dim red light from the rats (one to two animals per study group) 37 days post-injection and from all the rabbits before surgery and 15–17, 35–39, and 73–79 days after transplantation. Systemic and topical anesthesia and dilation of the pupils were performed as mentioned above (rabbits) or in S1 Materials and Methods (rats). ERG recordings were performed using a portable handheld multi-species

Electroretinograph Model 2000 Unit (HMsERG, OcuScience, NV, USA). The eyes were stimulated with a mini-Ganzfeld dome either bilaterally with both eyes inside the dome (rats) or unilaterally with the center of the dome positioned 2 cm from the tested eye (rabbits). As a recording electrode, an ERG-jet contact lens electrode with gold mylar film was used for rabbits and a silver-embedded thread electrode with mini contact lens for rats (both from OcuScience). The ground and reference electrodes were stainless steel needle electrodes.

The recordings were performed in a Faraday cage. In rabbits, the ground electrode was placed subcutaneously over the external occipital protuberance and the reference electrodes were placed a few centimeters caudal to the lateral canthus. In rats, the ground electrode was placed subcutaneously above the base of the tail and the reference electrodes were placed subcutaneously in each cheek. The recording electrodes were placed on the cornea with 2% methylcellulose. Scotopic flash ERGs were recorded at 1, 3, 10, 30, 100, 300, 1000, 3000, 10000, and 25000 mcds/m^2. Signals were amplified, digitized, averaged, and stored using ERGView 4.380R software (OcuScience). The analysis was performed with ERGView 4.380R software by evaluating the ERG waveforms as well as by measuring the amplitudes and implicit times for the a- and b-waves.

Three months after transplantation, OCT was performed to rabbits using Stratus OCT scanner, (Carl Zeiss Meditec, Dublin, CA, USA).

Retinal histology and immunohistochemistry. The animals were humanely euthanized at the end of the experiment with carbon dioxide (rats) or with overdose injection of pentobarbital sodium (rabbits). The eyes were fixed in Davidson's fixative and processed for paraffin embedding following standard techniques and cut into five-micron sections. For histology, specimens were conventionally stained with haematoxylin and eosin, and observed under a microscope (Nikon Instruments Europe, Amsterdam, Netherlands). ONL thickness was measured from three separate sections per eye with ImageJ Processing and Analysis Software [29]. A total of 10–12 measurements were taken per section. From manipulated eyes, 5–6 measurements were taken from the graft site and 5–6 distally from the graft site with 100–200 μm intervals.

For immunohistochemistry, the samples were deparaffinated, hydrated and stained using conventional protocols. Antigen retrieval was performed by boiling slides for 5 min in 0.01 M citrate buffer (pH 6.0). Primary antibody information is listed in S1 Table. Primary antibodies were diluted 1:50 (anti-CRALBP, anti-CD68, anti-CD3, anti-TRA-1-85) for overnight at +4°C. Alexa Fluor 568-conjugated donkey anti-mouse IgG and Alexa Fluor 488-conjugated donkey anti-goat IgG (both 1:400, Life Technologies) were used as secondary antibodies. Sections not incubated with primary antibodies served as negative controls. Images were taken using Olympus IX51 fluorescence microscope (Olympus, Tokyo, Japan).

Statistical analysis. Statistical analysis between two groups was performed with the unpaired Mann-Whitney U test using IBM SPSS Statistics software. A p value of < 0.05 was considered statistically significant.

Results

Suspension injection of hESC-RPE into rat eye

Prior injection, hESC-RPE cells expressed several RPE markers both at the RNA (S1A Fig) and protein (S1B Fig) level and did not show expression of pluripotency markers *OCT4* and *NANOG* RNA (S1A Fig). Majority of the cells were still alive in suspension at the time of injection based on live/dead staining (S1C Fig).

At day 37 post-injection, some functional rescue of ERG signal was detected in hESC-RPE injected dystrophic eyes (Fig 1) and in one animal ONL thickness was also significantly

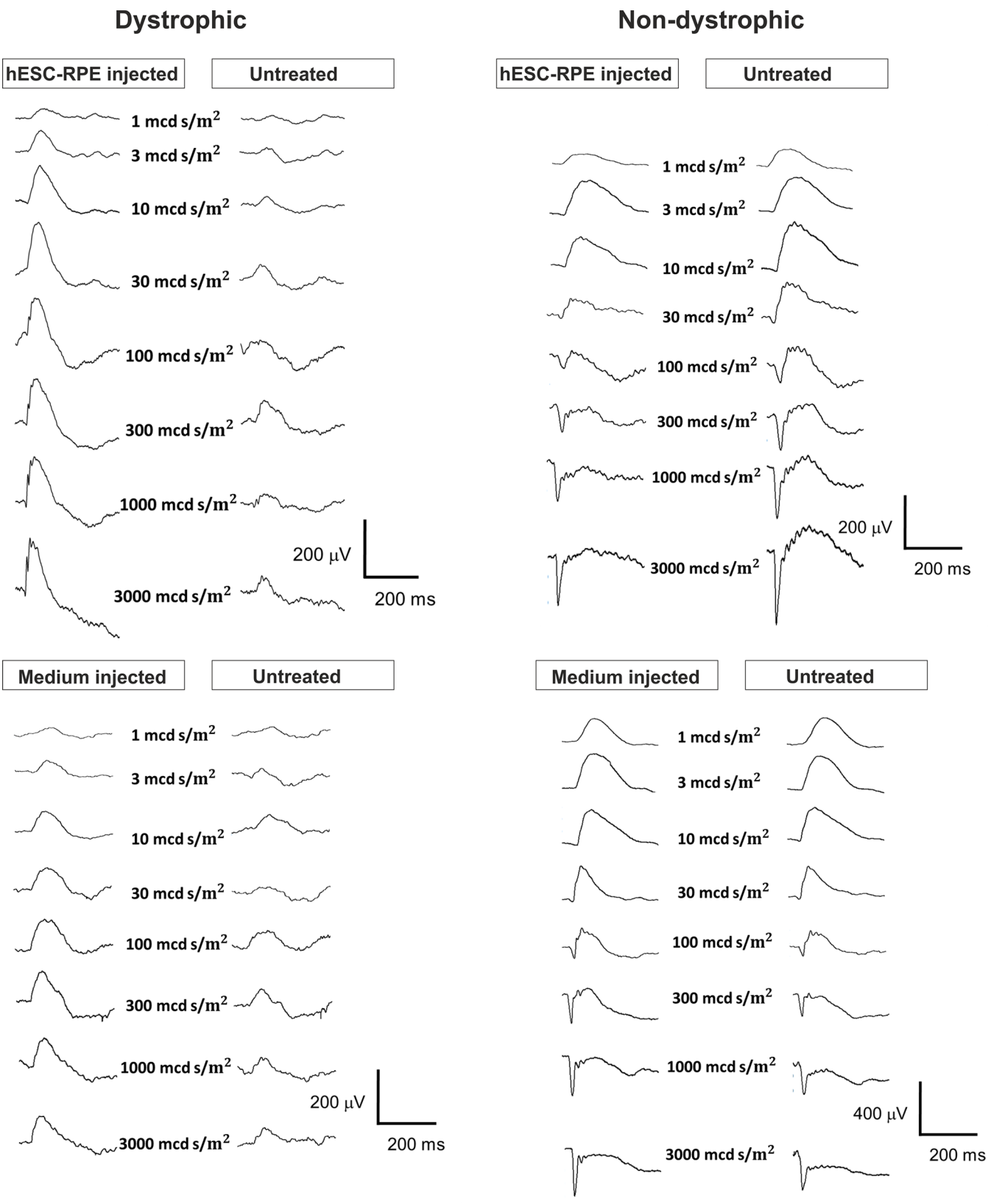
Dystrophic
hESC-RPE injected
Untreated
1 mcd s/m2
3 mcd s/m2
10 mcd s/m2
30 mcd s/m2
100 mcd s/m2
300 mcd s/m2
1000 mcd s/m2
3000 mcd s/m2
200 μV
200 ms
Non-dystrophic
hESC-RPE injected
Untreated
1 mcd s/m2
3 mcd s/m2
10 mcd s/m2
30 mcd s/m2
100 mcd s/m2
300 mcd s/m2
1000 mcd s/m2
3000 mcd s/m2
200 μV
200 ms
Medium injected
Untreated
1 mcd s/m2
3 mcd s/m2
10 mcd s/m2
30 mcd s/m2
100 mcd s/m2
300 mcd s/m2
1000 mcd s/m2
3000 mcd s/m2
200 μV
200 ms
Medium injected
Untreated
1 mcd s/m2
3 mcd s/m2
10 mcd s/m2
30 mcd s/m2
100 mcd s/m2
300 mcd s/m2
1000 mcd s/m2
3000 mcd s/m2
400 μV
200 ms

Fig 1. Dark-adapted ERG responses following subretinal injections in dystrophic and non-dystrophic RCS rats. Representative and averaged (2 to 20 responses) ERG recordings from dystrophic and non-dystrophic rats 37 days after subretinal injection of hESC-RPE or medium alone compared to the non-operated fellow eye.

doi:10.1371/journal.pone.0143669.g001

($p < 0.001$) preserved (Fig 2). Slight functional rescue (Fig 1) but no ONL preservation (Fig 2) was detected in the dystrophic eye injected with medium only. In non-dystrophic rats, the ERG response was slightly lowered in hESC-RPE injected eyes and slightly increased in medium injected eyes compared to non-injected parallel eyes (Fig 1), but no significant changes were observed in the ONL thickness (Fig 2). Human antigen TRA-1-85 staining showed that 41 days post-injection most of the injected cells were located subretinally in different sized cell clusters in all rats (Fig 3A). Injected hESC-RPE cells also remained positive for RPE marker CRALBP (Fig 3B). In dystrophic eyes, infiltration of CD68 positive cells was observed in the outer segment debris zone, also without injection (data not shown), and around the injected hESC-RPE cells (Fig 3C). In one of the dystrophic eyes, infiltration of CD3 positive cells was also present around the injected cells (Fig 3D). In non-dystrophic eyes, CD68 positive cells were detected in the subretinal space only in the hESC-RPE injected eyes, mainly around the injected cells and no CD3 positive cells were detected (data not shown). Clusters of large pigmented cells were present even after 105 days post-injection. However, these cells were not positive for TRA-1-85 or CRALBP. Instead, the pigmentation appeared to co-localize with CD68 staining (Fig 3E). No intraocular tumors were detected.

Surface and permeability characterization of ultrathin PI carrier

For subretinal sheet transplantation of hESC-RPE cells, the suitability of ultrathin PI membrane was examined. SEM was used to evaluate the average pore distribution of PI. PET

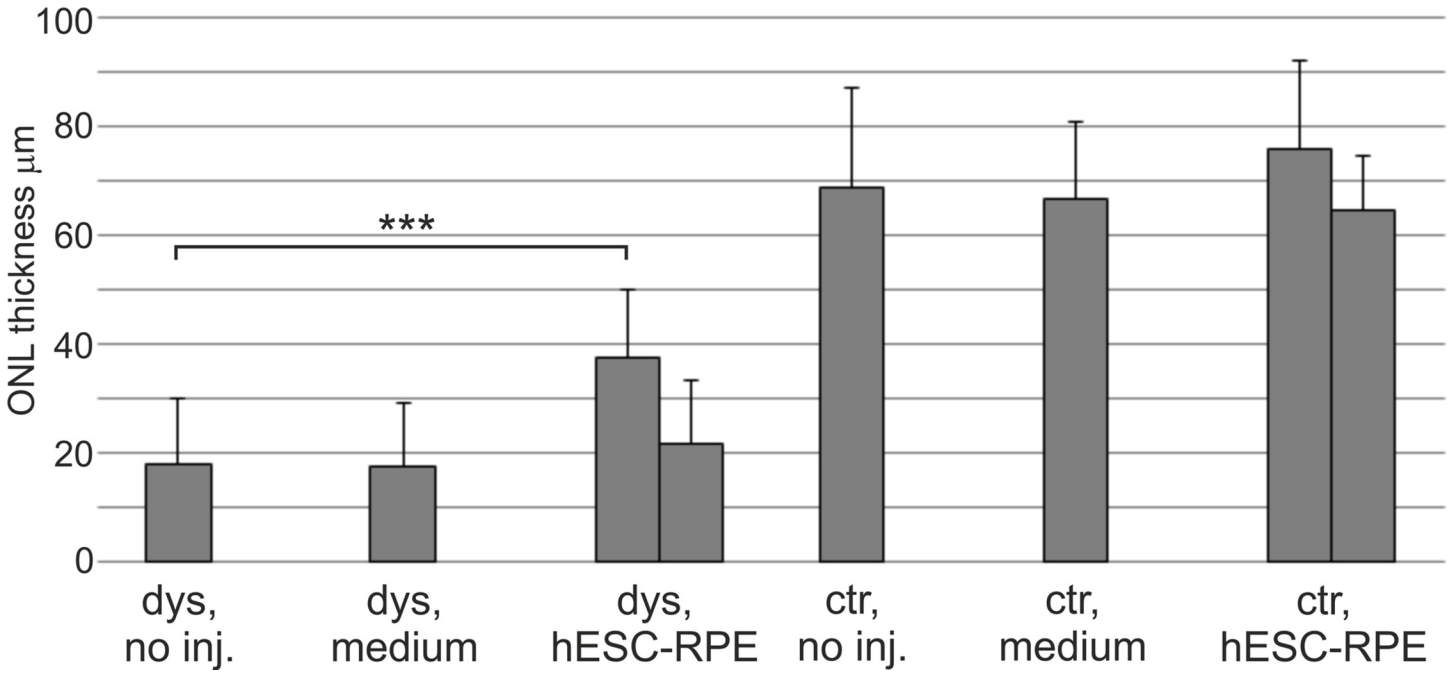

Fig 2. ONL thickness following subretinal injections in dystrophic and non-dystrophic RCS rats. ONL thicknesses were measured from HE samples of rats euthanized 41 days post-injection. Each column represents one rat eye. Measurements were performed with ImageJ software. Error bars show standard deviation.

doi:10.1371/journal.pone.0143669.g002

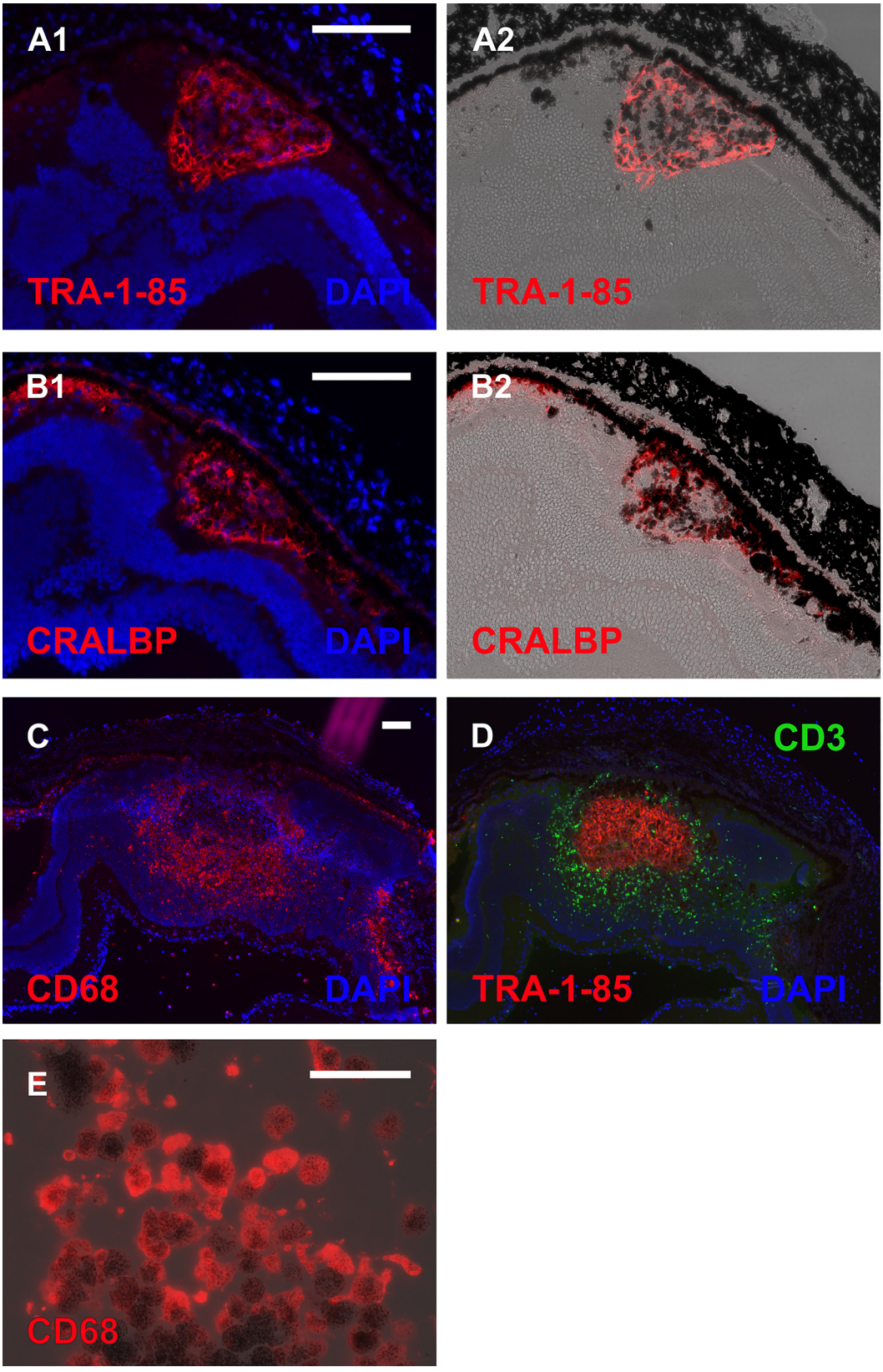
A1
TRA-1-85
DAPI
A2
TRA-1-85
B1
CRALBP
DAPI
B2
CRALBP
C
CD68
DAPI
D
CD3
TRA-1-85
DAPI
E
CD68

Fig 3. Implanted eyes of dystrophic RCS rats. Immunohistochemical staining showing labeling of injected cells 41 days post-injection with antibodies against human antigen TRA-1-85 (A1-2), RPE marker CRALBP (B1-2, antibody recognizes also rat CRALBP), macrophage marker CD68 (C), and T-cell marker CD3 (D). Large pigmented cells detected 105 days post-injection were positive for CD68 antibody (E). Scale bar 100 μm in A-D and 50 μm in E.

doi:10.1371/journal.pone.0143669.g003

membrane, a commonly used RPE culture substrate [18, 28, 30, 31], was analyzed for comparison. SEM showed that PI membranes had higher pore density compared to PET (Fig 4A). AFM revealed a clear nanotopography on both membranes (Fig 4B and 4C). PI had slightly rougher surface morphology (Rq 26.2±9.7 nm) compared to PET (Rq 13.5±3.8 nm). Contact angle measurements (Fig 4D) demonstrated slightly lower values in the surface wettability for PI (average 53.9±6.0°) compared to PET (average 70.6±6.4°). PI membranes also demonstrate higher Papp-value (2.34 x 10–4± 2.47 x 10–5 cm^2s^{-1}) compared to the Papp for PET (7.15 x 10–5±2.57 x 10–5 cm^2s^{-1}, Fig 4E) and larger increase in cumulative permeability of the small molecular weight substance over time. After four hours, PI membranes showed high cumulative permeability of 11.3±0.3%, whereas notably lower cumulative permeability of 3.0x0.9% was recorded for the PET membranes (Fig 4F).

PI membrane transplantation of hESC-RPE into rabbit eye

Apart from cataract formation in some of the rabbits, there were no other significant surgical complications. OCT showed good placement of the membranes (Fig 5A–5C). In one rabbit with hESC-RPE-PI some subretinal fluid on the membrane was detected (Fig 5C). A gradual loss of pigmentation on hESC-RPE-PI was observed over time (Fig 5D). Over two months, a-wave ERG responses remained roughly equal in eyes with hESC-RPE-PI or PI alone compared to the fellow eyes. In one rabbit with hESC-RPE-PI, the a-wave amplitude was clearly reduced in the operated eye (S2 Fig). On the other hand, after two months the b-wave amplitudes were clearly reduced in all eyes, operated and non-operated, compared to the amplitudes measured prior surgery (S2 Fig). At the three-month end point, ERG measurements were discarded due to cataract formation.

Three months after transplantation, histological analysis showed no evidence of intraocular tumors. In the surgical control or eyes with PI alone, no obvious signs of inflammation or significant retinal atrophy were observed (Fig 6A and 6B). However, in eyes transplanted with hESC-RPE-PI, mononuclear cell infiltration was observed around two out of five membranes and the ONL was totally destroyed (Fig 6C). In two out of five hESC-RPE-PI transplanted eyes, ONL was disorganized and the number of nuclei was reduced either over whole or part of the membrane (Fig 6D). In one eye with hESC-RPE-PI, the ONL thickness was only slightly reduced and ONL nuclear density was somewhat preserved compared to the areas away from the membrane (Fig 6E). Overall, ONL thickness was significantly ($p < 0.001$) reduced over hESC-RPE-PI compared to regions away from the membrane (Fig 6F).

The hESC-RPE-PI transplantations were performed with surgical forceps. In addition to difficulties in controlling the membrane during delivery, there is a high risk for damaging the hESC-RPE cells. Thus, we subsequently studied the use of a metallic shooter instrument with plain ultrathin PI. Despite multiple intraoperative attempts, delivery of the ultrathin PI proved incompatible with the shooter instrument in its current form as the membrane was too pliable, folded around the edges of the instrument during ejection or would be bend at the retinotomy.

Discussion

Differentiation of RPE cells from hPSCs have made cell therapy a potential treatment for RPE-related diseases [4, 32]. Recent clinical trials with hESC-RPE cell suspensions injected subretinally have so far reported no major adverse effects related to the transplanted cells [7, 8, 33].

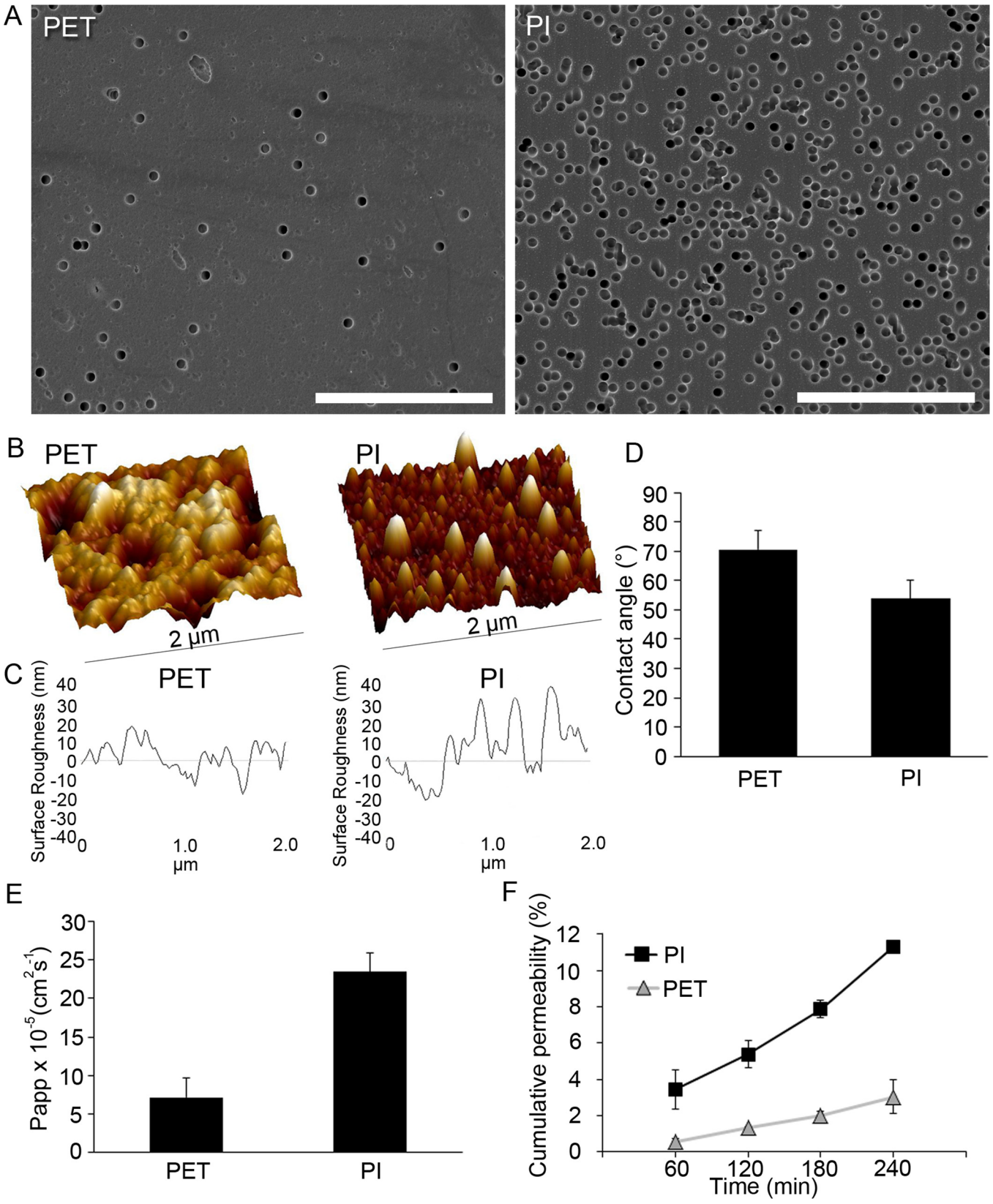
A
PET
PI
B
PET
PI
2 µm
2 µm
C
PET
PI
Surface Roughness (nm)
40
30
20
10
0
-10
-20
-30
-40
0
1.0
2.0
µm
D
Contact angle (°)
90
80
70
60
50
40
30
20
10
0
PET
PI
E
Papp x 10-5(cm2s-1)
30
25
20
15
10
5
0
PET
PI
F
Cumulative permeability (%)
12
10
8
6
4
2
0
PI
PET
60
120
180
240
Time (min)

Fig 4. PI and PET membrane surface and permeability characteristics. SEM micrographs of PET and PI surface topography and pore distribution, scale bars 20 μm (A). AFM 3D images (B) and line profiles (C) demonstrating the surface roughness of PET and PI. Contact angle measurements of PET and PI (D). The apparent permeability coefficient Papp (E) and the cumulative permeability of small molecular weight fluorescent marker (F) for the PET and PI.

doi:10.1371/journal.pone.0143669.g004

However, for successful treatment, the suspension transplanted cells need to adhere on the Bruch's membrane and be integrated into the existing RPE layer to escape cell death and potential immune rejection and to function properly. In the pathologic environment of diseased retina, reaching sufficient level of integration may prove to be a difficult task. It is known that RPE attaches poorly to diseased or aged Bruch's membrane [34–36]. In animal models, unattached cells have formed large cell clusters and the nonintegrated cells have been eventually cleared, potentially by macrophages [13, 37, 38]. Likewise, in our cell suspension experiments, the injected hESC-RPE cells were mainly detected in cell clusters and after 105 days no TRA-1-85 positive cells could be identified. Instead, the pigmented cells present stained with anti-CD68 being potentially macrophages which had engulfed the transplanted cells. Short-term, the hESC-RPE cells survived in the subretinal space and some functional rescue of ERG signals in the hESC-RPE injected dystrophic rat eyes was detected. Curiously, minor functional rescue/improvement of ERG signal was detected also in medium injected eyes in dystrophic and non-dystrophic rats. It is possible that e.g. macrophages potentially recruited to the injection site cause this effect by phagocytosis and/or secretion of trophic factors, thus promoting survival or function of the photoreceptors. Indeed, other cell types than RPE, such as mesenchymal stem cells, have shown similar protective effects following subretinal injection into RCS rats. The underlying mechanisms still remain mainly elusive, but recent data suggests that activation of endogenous regenerative mechanisms such as the progenitor potential of retinal Müller cells may play a role, in particular since a therapeutic benefit does not require the cells to persist in the transplantation site [39–42].

In order to increase the survival rate of the transplanted cells and to reconstruct or replace the damaged Bruch's membrane, efforts have been made to develop a suitable RPE-scaffold implant [13, 14, 16–20, 43]. The requirements for the scaffold include support of RPE monolayer growth and functionality, bio- and immune compatibility, and surgical manageability. Carrier porosity/permeability is important, especially if the scaffold is not rapidly biodegradable. Elastic modulus is another important parameter, not only to avoid problems like retinal detachment but to support proper RPE function like phagocytosis which has been shown to be decreased on firm substrates compared to more flexible ones [44]. To date, there have been no published large animal studies with transplantation of hPSC-derived RPE on a supportive scaffold. We have previously shown that PI is a suitable culture surface for hESC-RPE [25]. In the current study, we further examined the porosity and permeability of ultrathin PI and its suitability for subretinal transplantation. The pore density of the studied PI membranes was good and the pores were evenly distributed. In culture, no dome formation, a typical feature of transporting epithelia on non-permeable surfaces [45, 46], was detected on the PI membranes. PI was also well tolerated in the subretinal space. Since the examined PI membrane was very thin and flexible, it conformed well to the shape of the surrounding space and post-surgical retinal detachments were not observed. Due to the merangiotic nature of rabbit retina, most of the blood supply of the inner retina is derived from the choriocapillaris [47], which would likely lead to rapid retinal damage, if blocked by a non-permeable implant. In a previous study by Montezuma et al. 2006 [24], the authors reported disorganization of the ONL when non-perforated PI implants were transplanted in pigs, despite the fact that pigs have both choroidal and retinal arterial blood supply to the retina. In our study, the retinal nuclear layers were well preserved over the PI even three months post-transplantation, indicating good permeability and

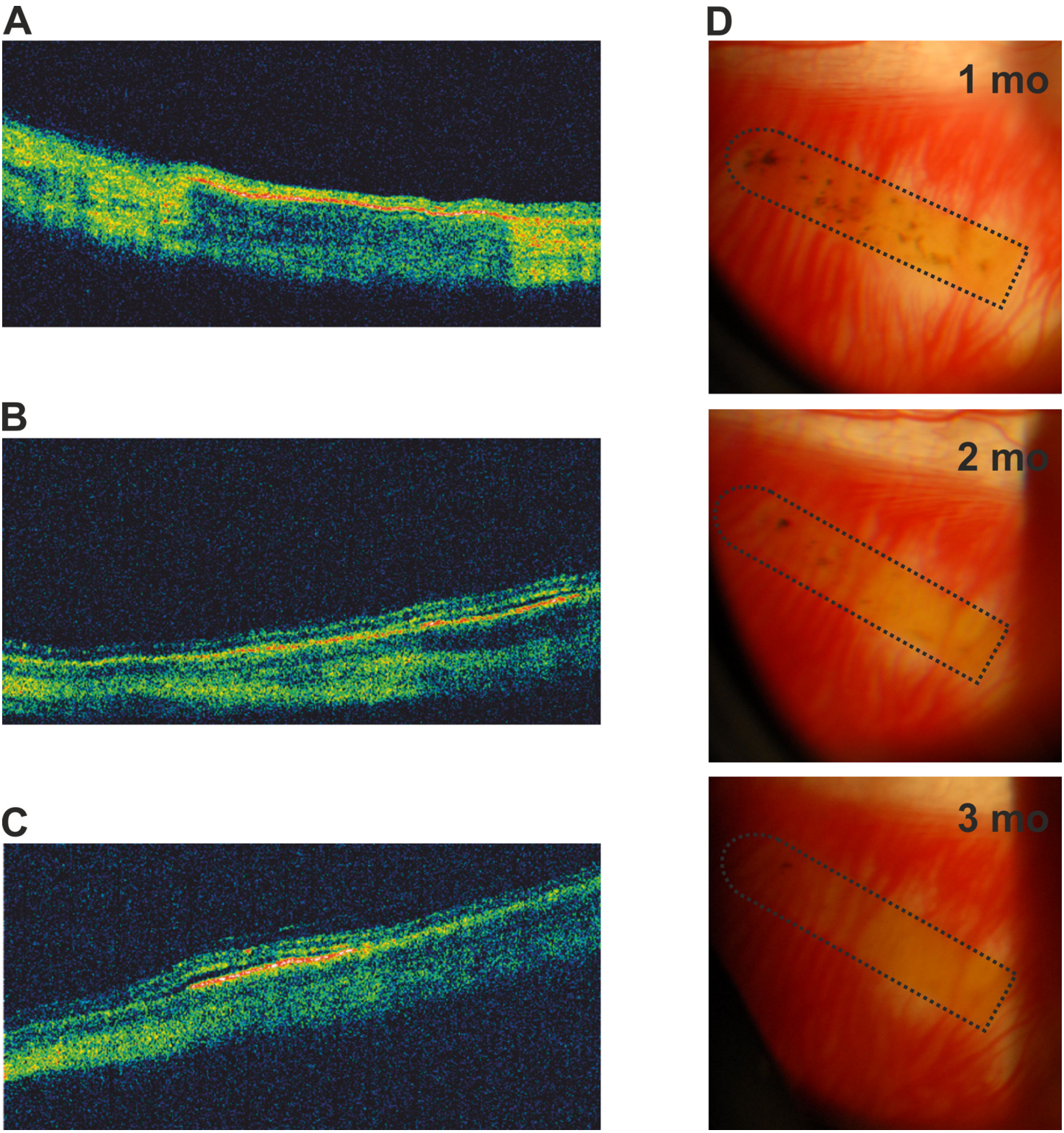

Fig 5. In vivo follow-up of hESC-RPE-PI implanted rabbit eyes. OCT scans showing hESC-RPE-PI in three different rabbit eyes three months after transplantation (A-C). Representative fundus photographs showing hESC-RPE-PI (marked with dotted line) of one rabbit one, two and three months after transplantation (D).

doi:10.1371/journal.pone.0143669.g005

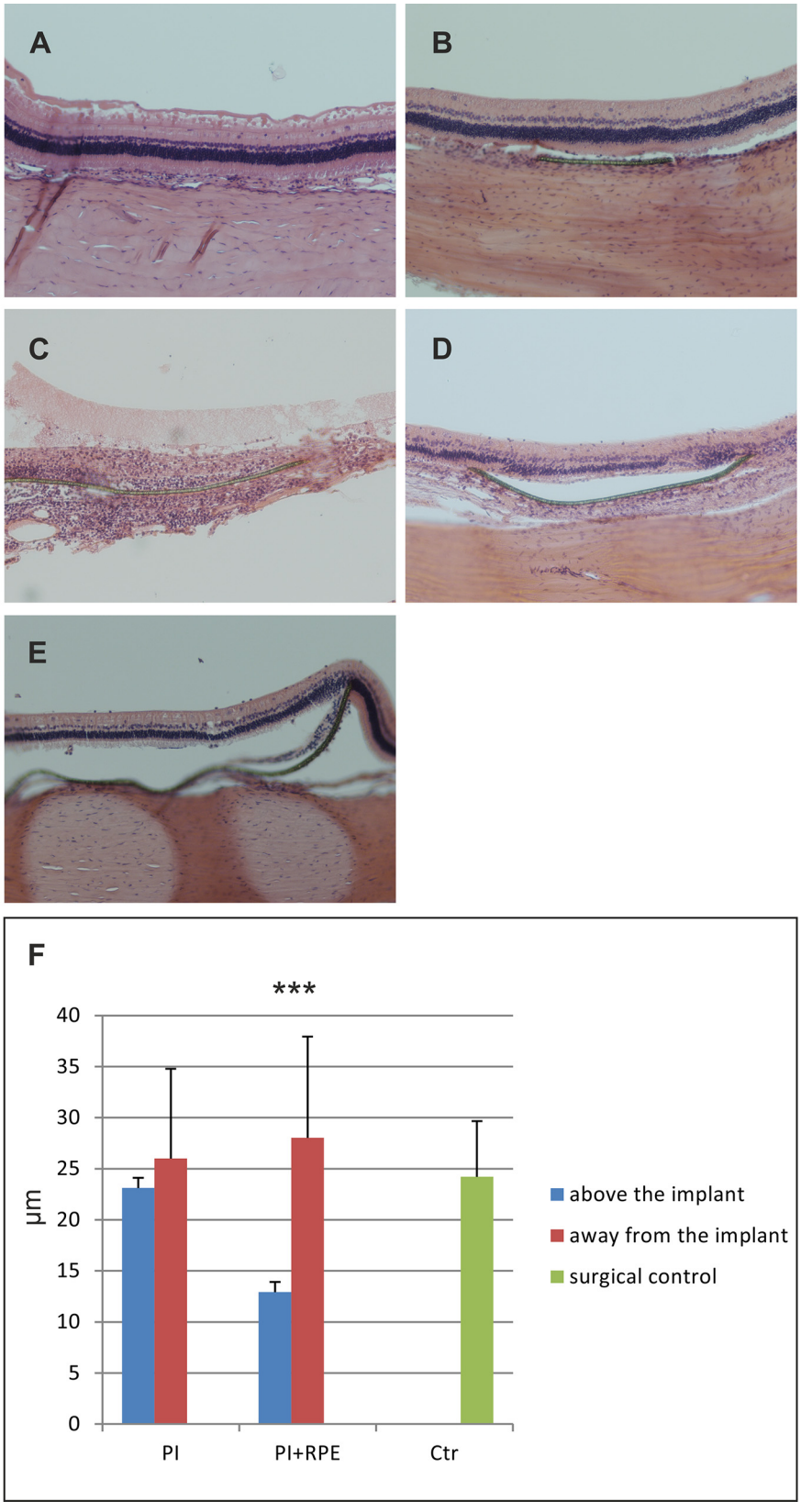
A
B
C
D
E
F
***
40
35
30
25
20
15
10
5
0
µm
PI
PI+RPE
Ctr
above the implant
away from the implant
surgical control

Fig 6. Histological analyses of rabbit retinas three months post-transplantation. HE staining of surgical control (A), PI alone (B) and hESC-RPE-PI (C and D). ONL thicknesses measured from HE samples, surgical control (n = 1), PI alone (n = 3), hESC-PI (n = 5) (E). Measurements were performed with ImageJ software. Error bars show standard deviation.

doi:10.1371/journal.pone.0143669.g006

biocompatibility. On the other hand, when hESC-RPE-PI were transplanted, varying level of disorganization of the ONL and loss of the photoreceptors were detected in most of the rabbits. In two out of five rabbits, there was mononuclear cell infiltration around the hESC-RPE-PI. We also noticed a gradual loss of pigmentation on the membranes, most likely due to the loss of hESC-RPE and not depigmentation since no TRA-1-85 positive cells were detected on the implants. Graft rejection in allogeneic and xenogeneic transplantations is a major obstacle. Although eye is considered as an immune privileged organ and RPE as immunomodulatory tissue, subretinal transplantation experiments with both allografts and xenografts in several animal models have demonstrated that the immunological privilege of the subretinal space is imperfect or may be easily compromised [13, 34, 37, 48, 49]. Recent studies indicate, that transplanted allogeneic iPSC-RPE cells induce an innate immune response which cannot be overcome by the immunomodulatory mechanisms in the eye [11, 49]. One major factor in ocular immune privilege is the blood-retina barrier [50]. This barrier may be broken by diseases, such as AMD, or surgical procedure, exposing the transplanted tissue to immune rejection. Although hPSCs express low levels of MHC-I and β2-microglobin at their surface, expression of these proteins increases upon RPE differentiation. The cells may also acquire immunogenic features during prolonged culture, especially if exposed to xeno-products and undefined factors, such as serum [51–53]. Additionally, exposure of iPSC-RPE cells to proinflammatory cytokine interferon-gamma increases their MHC-II expression. These factors can predispose allogeneic implants to immune rejection of [11]. In our study, immunosuppressant was administered in the drinking water. This may be problematic, because water consumption of the animals varied substantially (daily intake of each animal was between 3%-100% of total water volume) leading potentially to variation in the cyclosporine plasma levels. As we did not examine this, insufficient immunosuppression could at least partly explain the loss of transplanted cells. The type and dose of immunosuppressant, administration route, and duration of immunosuppression remain to be studied further. It may also be, that by using autologous iPSC-RPE cells no immunosuppression is needed, as these cells seem to be immune tolerated [11, 54]. For future therapeutical use, ability to reduce the immunogenicity of allogeneic cultured RPE cells, or use of autologous or HLA-homozygous hiPSCs for better immunological compatibility, would greatly facilitate the application of hPSC-based RPE cells therapies.

Surgical manageability is an important factor contributing to the success of transplantation. In the study by Diniz *et al.* 2013, hESC-RPE were transplanted as a sheets on ultrathin parylene membranes into the subretinal space of rats. Many of the complications detected in their study, including damage to the transplanted RPE and increased cell reaction at the implant area, could potentially be explained by the surgical technique involving choroidal incision commonly used in animals with small eyes and large crystalline lenses [13]. In our study rabbit was chosen as the model animal due to its larger eye size allowing the use of surgical techniques similar to clinical procedures. However, although the biocompatibility of the ultrathin PI was good, the surgical technique still requires further development. During the hESC-RPE-PI transplantations, the membrane was exposed, potentially leading to damage to the hESC-RPE. To protect the cells, we tested the use of a shooter instrument with ultrathin PI. However, in their present forms, the ultrathin PI and the shooter instrument were not compatible as PI was too flexible. Flexibility is a typical problem also with other ultrathin substrates, such as parylene [20]. Further modifications to improve the surgical manageability of the ultrathin PI

membrane would facilitate its usefulness in the future. Such enforcement could e.g. be added as a transient feature, by encapsulating the implant into rapidly biodegradable hydrogel. Alternatively delivery strategies may comprise injection through BSS or viscoelastic, in analogy to the approach by the Japanese hiPSC-RPE clinical trial [11].

Safety of transplanting cells differentiated from PSCs remains an important aspect. Although so far in the animal and human trials no major concerns have arisen, the safety of hPSC-derived cells in therapeutical use awaits final confirmation. In our study, the transplanted cells did no longer express pluripotency markers *OCT4* and *NANOG*. Additionally, no major adverse effects such as tumor formation were detected either in the rat or rabbit eyes.

In summary, ultrathin, porous PI was well tolerated in the subretinal space and preservation of ONL was observed even after three months of transplantation. We believe, that with proper modifications and protection of the RPE during transplantation, ultrathin PI is a promising scaffold material for therapeutic subretinal transplantation of RPE cells.

Supporting Information

S1 Fig. Gene and protein expression profiles of hESC-RPE prior injection into rats. RT–PCR analysis of eye/RPE and pluripotency marker genes, genomic control reactions excluding the enzyme are marked '-RT' (A). Cytospin preparations showing the immunocytochemical staining of RPE/eye markers bestrophin-1, MITF, CRALBP, and PAX6, scale bar 50 μm (B). Live/Dead cell viability assay showing live cells stained with Calcein-AM (green) and dead cells with EthD-1 (red), scale bar 100 μm (C).
(TIF)

S2 Fig. Dark-adapted ERG responses following PI transplantation into rabbit eyes. Fig shows averaged (two responses) flash ERGs recorded at 25 000 mcds/m^2. Responses measured prior operation are in black and responses two months after transplantation are in red.
(TIF)

S1 Materials and Methods.
(DOCX)

S1 Table. Primary antibody information.
(DOCX)

S2 Table. RT-PCR Primer sequences.
(DOCX)

Acknowledgments

The authors wish to thank Pirjo Nelimarkka-Niinimäki, Marja Mali, Johanna Nuto, Outi Melin, Outi Heikkilä, Hanna Pekkanen, Marja-Leena Koskinen, Monica Nieminen, Ulla Aapola, Jussi Muranen, and Prof. George Burke's group (University of Ulster, Northern Ireland) for technical assistance, Prof. Peter Andrews (University of Sheffield, UK) for providing the TRA-1-85 antibody, and Prof. Robin Ali (UCL Institute of Ophthalmology, London, UK) for providing the RCS rats. Additionally, the authors wish to thank Prof. Arto Urtti and Prof. Kai Kaarniranta for their scientific expertise for this work.

Author Contributions

Conceived and designed the experiments: TI HH PK SN AS J-HW BS HU HS. Performed the experiments: TI HH PK SN AS J-HW BS FT. Analyzed the data: TI HH PK SN AS BS FT HU.

Contributed reagents/materials/analysis tools: BS PA OO MK HU HS. Wrote the paper: TI HH PK SN AS BS PA HU HS.

References

1. Strauss O. The retinal pigment epithelium in visual function. Physiol Rev 2005 Jul; 85(3):845–881. PMID: 15987797
2. Klein R, Klein BE. The prevalence of age-related eye diseases and visual impairment in aging: current estimates. Invest Ophthalmol Vis Sci 2013 Dec 13; 54(14):ORSF5–ORSF13. doi: 10.1167/iovs.13-12789 PMID: 24335069
3. Sparrow JR, Hicks D, Hamel CP. The retinal pigment epithelium in health and disease. Curr Mol Med 2010 Dec; 10(9):802–823. PMID: 21091424
4. Dang Y, Zhang C, Zhu Y. Stem cell therapies for age-related macular degeneration: the past, present, and future. Clin Interv Aging 2015 Jan 14; 10:255–264. doi: 10.2147/CIA.S73705 PMID: 25609937
5. Rowland TJ, Buchholz DE, Clegg DO. Pluripotent human stem cells for the treatment of retinal disease. J Cell Physiol 2012 Feb; 227(2):457–466. doi: 10.1002/jcp.22814 PMID: 21520078
6. Bharti K, Rao M, Hull SC, Stroncek D, Brooks BP, Feigal E, et al. Developing cellular therapies for retinal degenerative diseases. Invest Ophthalmol Vis Sci 2014 Feb 26; 55(2):1191–1202. doi: 10.1167/iovs.13-13481 PMID: 24573369
7. Schwartz SD, Hubschman JP, Heilwell G, Franco-Cardenas V, Pan CK, Ostrick RM, et al. Embryonic stem cell trials for macular degeneration: a preliminary report. Lancet 2012 Feb 25; 379(9817):713–720. doi: 10.1016/S0140-6736(12)60028-2 PMID: 22281388
8. Schwartz SD, Regillo CD, Lam BL, Eliott D, Rosenfeld PJ, Gregori NZ, et al. Human embryonic stem cell-derived retinal pigment epithelium in patients with age-related macular degeneration and Stargardt's macular dystrophy: follow-up of two open-label phase 1/2 studies. Lancet 2015 Feb 7; 385(9967):509–516. doi: 10.1016/S0140-6736(14)61376-3 PMID: 25458728
9. Sugino IK, Rapista A, Sun Q, Wang J, Nunes CF, Cheewatrakoolpong N, et al. A method to enhance cell survival on Bruch's membrane in eyes affected by age and age-related macular degeneration. Invest Ophthalmol Vis Sci 2011 Dec 20; 52(13):9598–9609. doi: 10.1167/iovs.11-8400 PMID: 22039244
10. Heller JP, Martin KR. Enhancing RPE Cell-Based Therapy Outcomes for AMD: The Role of Bruch's Membrane. Transl Vis Sci Technol 2014 Jul 3; 3(3):11. PMID: 25068093
11. Kamao H, Mandai M, Okamoto S, Sakai N, Suga A, Sugita S, et al. Characterization of human induced pluripotent stem cell-derived retinal pigment epithelium cell sheets aiming for clinical application. Stem Cell Reports 2014 Jan 23; 2(2):205–218. doi: 10.1016/j.stemcr.2013.12.007 PMID: 24527394
12. Kanemura H, Go MJ, Shikamura M, Nishishita N, Sakai N, Kamao H, et al. Tumorigenicity studies of induced pluripotent stem cell (iPSC)-derived retinal pigment epithelium (RPE) for the treatment of age-related macular degeneration. PLoS One 2014 Jan 14; 9(1):e85336. doi: 10.1371/journal.pone.0085336 PMID: 24454843
13. Diniz B, Thomas P, Thomas B, Ribeiro R, Hu Y, Brant R, et al. Subretinal implantation of retinal pigment epithelial cells derived from human embryonic stem cells: improved survival when implanted as a monolayer. Invest Ophthalmol Vis Sci 2013 Jul 26; 54(7):5087–5096. doi: 10.1167/iovs.12-11239 PMID: 23833067
14. Hynes SR, Lavik EB. A tissue-engineered approach towards retinal repair: scaffolds for cell transplantation to the subretinal space. Graefes Arch Clin Exp Ophthalmol 2010 Jun; 248(6):763–778. doi: 10.1007/s00417-009-1263-7 PMID: 20169358
15. Liu Z, Yu N, Holz FG, Yang F, Stanzel BV. Enhancement of retinal pigment epithelial culture characteristics and subretinal space tolerance of scaffolds with 200 nm fiber topography. Biomaterials 2014 Mar; 35(9):2837–2850. doi: 10.1016/j.biomaterials.2013.12.069 PMID: 24439407
16. Sorkio AE, Vuorimaa-Laukkanen EP, Hakola HM, Liang H, Ujula TA, Valle-Delgado JJ, et al. Biomimetic collagen I and IV double layer Langmuir-Schaefer films as microenvironment for human pluripotent stem cell derived retinal pigment epithelial cells. Biomaterials 2015 May; 51:257–269. doi: 10.1016/j.biomaterials.2015.02.005 PMID: 25771016
17. Sorkio A, Porter PJ, Juuti-Uusitalo K, Meenan BJ, Skottman H, Burke GA. Surface Modified Biodegradable Electrospun Membranes as a Carrier for Human Embryonic Stem Cell-Derived Retinal Pigment Epithelial Cells. Tissue Eng Part A 2015 Jun 30.
18. Stanzel BV, Liu Z, Somboonthanakij S, Wongsawad W, Brinken R, Eter N, et al. Human RPE stem cells grown into polarized RPE monolayers on a polyester matrix are maintained after grafting into

rabbit subretinal space. Stem Cell Reports 2014 Jan 2; 2(1):64–77. doi: 10.1016/j.stemcr.2013.11.005 PMID: 24511471

19. Stanzel BV, Liu Z, Brinken R, Braun N, Holz FG, Eter N. Subretinal delivery of ultrathin rigid-elastic cell carriers using a metallic shooter instrument and biodegradable hydrogel encapsulation. Invest Ophthalmol Vis Sci 2012 Jan 31; 53(1):490–500. doi: 10.1167/iovs.11-8260 PMID: 22167099
20. Hu Y, Liu L, Lu B, Zhu D, Ribeiro R, Diniz B, et al. A novel approach for subretinal implantation of ultrathin substrates containing stem cell-derived retinal pigment epithelium monolayer. Ophthalmic Res 2012; 48(4):186–191. doi: 10.1159/000338749 PMID: 22868580
21. Kane FE, Burdan J, Cutino A, Green KE. Iluvien: a new sustained delivery technology for posterior eye disease. Expert Opin Drug Deliv 2008 Sep; 5(9):1039–1046. doi: 10.1517/17425247.5.9.1039 PMID: 18754752
22. Besch D, Sachs H, Szurman P, Gulicher D, Wilke R, Reinert S, et al. Extraocular surgery for implantation of an active subretinal visual prosthesis with external connections: feasibility and outcome in seven patients. Br J Ophthalmol 2008 Oct; 92(10):1361–1368. doi: 10.1136/bjo.2007.131961 PMID: 18662916
23. Julien S, Peters T, Ziemssen F, Arango-Gonzalez B, Beck S, Thielecke H, et al. Implantation of ultrathin, biofunctionalized polyimide membranes into the subretinal space of rats. Biomaterials 2011 Jun; 32(16):3890–3898. doi: 10.1016/j.biomaterials.2011.02.016 PMID: 21388675
24. Montezuma SR, Loewenstein J, Scholz C, Rizzo JF 3rd. Biocompatibility of materials implanted into the subretinal space of Yucatan pigs. Invest Ophthalmol Vis Sci 2006 Aug; 47(8):3514–3522. PMID: 16877423
25. Subrizi A, Hiidenmaa H, Ilmarinen T, Nymark S, Dubruel P, Uusitalo H, et al. Generation of hESC-derived retinal pigment epithelium on biopolymer coated polyimide membranes. Biomaterials 2012 Nov; 33(32):8047–8054. doi: 10.1016/j.biomaterials.2012.07.033 PMID: 22892561
26. LaVail MM. Legacy of the RCS rat: impact of a seminal study on retinal cell biology and retinal degenerative diseases. Prog Brain Res 2001; 131:617–627. PMID: 11420975
27. Skottman H. Derivation and characterization of three new human embryonic stem cell lines in Finland. In Vitro Cell Dev Biol Anim 2010 Apr; 46(3–4):206–209. doi: 10.1007/s11626-010-9286-2 PMID: 20177999
28. Vaajasaari H, Ilmarinen T, Juuti-Uusitalo K, Rajala K, Onnela N, Narkilahti S, et al. Toward the defined and xeno-free differentiation of functional human pluripotent stem cell-derived retinal pigment epithelial cells. Mol Vis 2011 Feb 22; 17:558–575. PMID: 21364903
29. Schneider CA, Rasband WS, Eliceiri KW. NIH Image to ImageJ: 25 years of image analysis. Nat Methods 2012 Jul; 9(7):671–675. PMID: 22930834
30. Nistor G, Seiler MJ, Yan F, Ferguson D, Keirstead HS. Three-dimensional early retinal progenitor 3D tissue constructs derived from human embryonic stem cells. J Neurosci Methods 2010 Jun 30; 190 (1):63–70. doi: 10.1016/j.jneumeth.2010.04.025 PMID: 20447416
31. Peng S, Rao VS, Adelman RA, Rizzolo LJ. Claudin-19 and the barrier properties of the human retinal pigment epithelium. Invest Ophthalmol Vis Sci 2011 Mar 14; 52(3):1392–1403. doi: 10.1167/iovs.10-5984 PMID: 21071746
32. Forest DL, Johnson LV, Clegg DO. Cellular models and therapies for age-related macular degeneration. Dis Model Mech 2015 May 1; 8(5):421–427. doi: 10.1242/dmm.017236 PMID: 26035859
33. Song WK, Park KM, Kim HJ, Lee JH, Choi J, Chong SY, et al. Treatment of macular degeneration using embryonic stem cell-derived retinal pigment epithelium: preliminary results in asian patients. Stem Cell Reports 2015 May 12; 4(5):860–872. doi: 10.1016/j.stemcr.2015.04.005 PMID: 25937371
34. Del Priore LV, Tezel TH. Reattachment rate of human retinal pigment epithelium to layers of human Bruch's membrane. Arch Ophthalmol 1998 Mar; 116(3):335–341. PMID: 9514487
35. Gullapalli VK, Sugino IK, Van Patten Y, Shah S, Zarbin MA. Impaired RPE survival on aged submacular human Bruch's membrane. Exp Eye Res 2005 Feb; 80(2):235–248. PMID: 15670802
36. Sugino IK, Sun Q, Wang J, Nunes CF, Cheewatrakoolpong N, Rapista A, et al. Comparison of FRPE and human embryonic stem cell-derived RPE behavior on aged human Bruch's membrane. Invest Ophthalmol Vis Sci 2011 Jul 1; 52(8):4979–4997. doi: 10.1167/iovs.10-5386 PMID: 21460262
37. Carr AJ, Vugler AA, Hikita ST, Lawrence JM, Gias C, Chen LL, et al. Protective effects of human iPS-derived retinal pigment epithelium cell transplantation in the retinal dystrophic rat. PLoS One 2009 Dec 3; 4(12):e8152. doi: 10.1371/journal.pone.0008152 PMID: 19997644
38. Del Priore LV, Tezel TH, Kaplan HJ. Survival of allogeneic porcine retinal pigment epithelial sheets after subretinal transplantation. Invest Ophthalmol Vis Sci 2004 Mar; 45(3):985–992. PMID: 14985321

39. Lu B, Wang S, Girman S, McGill T, Ragaglia V, Lund R. Human adult bone marrow-derived somatic cells rescue vision in a rodent model of retinal degeneration. Exp Eye Res 2010 Sep; 91(3):449–455. doi: 10.1016/j.exer.2010.06.024 PMID: 20603115

40. Jian Q, Li Y, Yin ZQ. Rat BMSCs initiate retinal endogenous repair through NGF/TrkA signaling. Exp Eye Res 2015 Mar; 132:34–47. doi: 10.1016/j.exer.2015.01.008 PMID: 25584870

41. Inoue Y, Iriyama A, Ueno S, Takahashi H, Kondo M, Tamaki Y, et al. Subretinal transplantation of bone marrow mesenchymal stem cells delays retinal degeneration in the RCS rat model of retinal degeneration. Exp Eye Res 2007 Aug; 85(2):234–241. PMID: 17570362

42. Tzameret A, Sher I, Belkin M, Treves AJ, Meir A, Nagler A, et al. Transplantation of human bone marrow mesenchymal stem cells as a thin subretinal layer ameliorates retinal degeneration in a rat model of retinal dystrophy. Exp Eye Res 2014 Jan; 118:135–144. doi: 10.1016/j.exer.2013.10.023 PMID: 24239509

43. Thumann G, Viethen A, Gaebler A, Walter P, Kaempf S, Johnen S, et al. The in vitro and in vivo behaviour of retinal pigment epithelial cells cultured on ultrathin collagen membranes. Biomaterials 2009 Jan; 30(3):287–294. doi: 10.1016/j.biomaterials.2008.09.039 PMID: 18929407

44. Boochoon KS, Manarang JC, Davis JT, McDermott AM, Foster WJ. The influence of substrate elastic modulus on retinal pigment epithelial cell phagocytosis. J Biomech 2014 Sep 22; 47(12):3237–3240. doi: 10.1016/j.jbiomech.2014.06.021 PMID: 25016484

45. Sugahara K, Caldwell JH, Mason RJ. Electrical currents flow out of domes formed by cultured epithelial cells. J Cell Biol 1984 Oct; 99(4 Pt 1):1541–1544. PMID: 6480702

46. Pfeffer BA, Clark VM, Flannery JG, Bok D. Membrane receptors for retinol-binding protein in cultured human retinal pigment epithelium. Invest Ophthalmol Vis Sci 1986 Jul; 27(7):1031–1040. PMID: 3013795

47. Ninomiya H, Inomata T, Kanemaki N. Microvascular architecture of the rabbit eye: a scanning electron microscopic study of vascular corrosion casts. J Vet Med Sci 2008 Sep; 70(9):887–892. PMID: 18840961

48. Xian B, Huang B. The immune response of stem cells in subretinal transplantation. Stem Cell Res Ther 2015 Sep 14; 6(1):161-015-0167-1.

49. Sohn EH, Jiao C, Kaalberg E, Cranston C, Mullins RF, Stone EM, et al. Allogenic iPSC-derived RPE cell transplants induce immune response in pigs: a pilot study. Sci Rep 2015 Jul 3; 5:11791. doi: 10.1038/srep11791 PMID: 26138532

50. Zhou R, Caspi RR. Ocular immune privilege. F1000 Biol Rep 2010 Jan 18; 2: doi: 10.3410/B2-3 PMID: 20948803

51. Martin MJ, Muotri A, Gage F, Varki A. Human embryonic stem cells express an immunogenic nonhuman sialic acid. Nat Med 2005 Feb; 11(2):228–232. PMID: 15685172

52. Sakamoto N, Tsuji K, Muul LM, Lawler AM, Petricoin EF, Candotti F, et al. Bovine apolipoprotein B-100 is a dominant immunogen in therapeutic cell populations cultured in fetal calf serum in mice and humans. Blood 2007 Jul 15; 110(2):501–508. PMID: 17395779

53. Zakrzewski JL, van den Brink MR, Hubbell JA. Overcoming immunological barriers in regenerative medicine. Nat Biotechnol 2014 Aug; 32(8):786–794. doi: 10.1038/nbt.2960 PMID: 25093888

54. Zhao T, Zhang ZN, Westenskow PD, Todorova D, Hu Z, Lin T, et al. Humanized Mice Reveal Differential Immunogenicity of Cells Derived from Autologous Induced Pluripotent Stem Cells. Cell Stem Cell 2015 Sep 3; 17(3):353–359. doi: 10.1016/j.stem.2015.07.021 PMID: 26299572